Carbohydrate Polymers 90 (2012) 181–188

Contents lists available at SciVerse ScienceDirect

Carbohydrate Polymers

journal homepage: www.elsevier.com/locate/carbpol

Fabrication of electrospun biocomposites comprising polycaprolactone/fucoidan for tissue regeneration

Ji Seok Lee [a], Gyu Hyun Jin [a], Myung Gu Yeo [a], Chul Ho Jang [b], Haengnam Lee [a,*], Geun Hyung Kim [a,*]

[a] Bio/Nanofluidics Lab, Department of Mechanical Engineering, Chosun University, Gwangju, Republic of Korea
[b] Department of Otolaryngology, Chonnam National University Hospital, Gwangju, Republic of Korea

ARTICLE INFO

Article history:
Received 13 February 2012
Received in revised form 16 April 2012
Accepted 4 May 2012
Available online 11 May 2012

Keywords:
Fucoidan
Polycaprolactone
Biocomposite
Bone
Tissue regeneration

ABSTRACT

In this study, we designed a new biocomposite comprising electrospun polycaprolactone (PCL)/fucoidan, in which the fucoidan has various beneficial biological functions, including anticoagulant, antiviral, and immunomodulatory activity. To obtain the composite scaffolds, a mixture of PCL and fucoidan was electrospun using various compositions (1, 2, 3, and 10 wt.%) of fucoidan powders. The resultant electrospun composites exhibited improved tensile modulus and strength for limited weight fractions (<10 wt.%) of fucoidan when compared with the pure PCL fiber mats. In addition, the biocomposites showed dramatic hydrophilic properties at >3 wt.% of fucoidan in the PCL/fucoidan. The biocompatibility of the electrospun mats was examined *in vitro* using osteoblast-like cells (MG63). Total protein content, alkaline phosphatase activity, and calcium mineralization were assessed. Scanning electron microscopic images showed that the cells were distributed more widely and were agglomerated on PCL/fucoidan mats compared with pure PCL mats. In addition, total protein content, alkaline phosphatase activity, and calcium mineralization were higher with PCL/fucoidan mats than with pure PCL mats. These observations suggest that fucoidan-supplemented biocomposites would make excellent materials for tissue-engineering applications.

1. Introduction

Tissue engineering is a well known interdisciplinary research field that combines engineering, material science, and life sciences, including pharmacy, medical science, physiology, and others. The goal of tissue engineering is to replace or regenerate various tissues or organs that may have been damaged by trauma, tumors, or abnormal defects with various alternative substitutes (scaffolds). Recently, these scaffolds have been widely researched because they can significantly affect cell growth and differentiation, and the scaffolds have been combined with various drug delivery systems (Hirose, Amiya, Hirokawa, & Tanaka, 1987; Hubbell & Langer, 1995; Nerem & Sambanis, 1995; Ratner, Hoffman, Schoen, & Lemons, 1996; Yang, Leong, Du, & Chua, 2001; Yoo & Lee, 1998, chap. 2; Zeltinger, Sherwood, Graham, Mueller, & Griffith, 2001).

Ideal biomedical scaffolds should induce high cellular activities, have a large surface area to provide good attachment and proliferation of cells, have low toxicity, have low inflammatory properties, and have proper mechanical properties. In addition, they should be biodegradable to allow for replacement with neo-tissues and should be biocompatible during the degradation process (Chen, Ushida, & Tateishi, 2002; Hollister, 2005; Hutmacher, 2001; Kretlow & Mikos, 2008; Langer & Vacanti, 1993, 1995; Li, Laurencin, Caterson, Tuan, & Ko, 2002; Sachlos & Czernuszka, 2003).

One of the techniques used to fabricate biomedical scaffolds, electrospinning, is a typical electrohydrodynamic process that generates micro/nanofibers from various polymeric solutions under electric field conditions. This technique has several advantages, such as simplicity, ease, low cost of equipment, widely selective materials, and easy injection of various additives compared with other techniques (Ma, He, Yong, & Ramakrishna, 2005; Teo & Ramakrishna, 2006; Yoshimoto, Shin, Terai, & Vacanti, 2003). In addition, as a biomedical scaffold, electrospun micro/nanofibers are promising materials because their size and morphology are similar to components of the extracellular matrix (ECM), which functions to support a combination of tissues and has a high surface area and good mechanical properties to support neo-tissues. For these reasons, studies on electrospun micro/nanofibers mimicking the ECM have been widely conducted (Ma, Kotaki, Inai, & Ramakrishna, 2005; Shin, Yoshimoto, & Vacanti, 2004).

Poly(ε-caprolactone) (PCL) has been widely applied to fabricate biomedical scaffolds because of its controllable biodegradability, biocompatibility, easy processability, and good mechanical properties, but it has low initial cell attachment and proliferation because of its hydrophobicity and low inclusion of various cell growth

* Corresponding authors. Tel.: +82 62 230 7180; fax: +82 62 236 1534.
E-mail addresses: hnalee@chosun.ac.kr (H. Lee), gkim@chosun.ac.kr (G.H. Kim).

0144-8617/$ – see front matter © 2012 Elsevier Ltd. All rights reserved.
http://dx.doi.org/10.1016/j.carbpol.2012.05.012

factors (Glowacki & Mizuno, 2008). To overcome these deficiencies of PCL, we accommodated a new natural material, fucoidan, which is extracted from brown algae. Fucoidan is an anionic polysaccharide comprising fucose and sulfate ester groups (Li, Lu, Wei, & Zhao, 2008) as a reinforcing component of cellular activities for bone regeneration. In general, fucoidan can induce FGF-2 activity, assist fibrillar collagen matrix formation, enhance fibroblastic proliferation, and stimulate *in vitro* and *in vivo* angiogenesis (Luyt et al., 2003; Nakamura et al., 2008; Senni et al., 2003). As reported in several studies, although fucoidan may strongly affect cellular activities, one major obstacle is that it is very difficult to fabricate structured scaffolds because it is very soluble in water.

For these reasons, we aimed to fabricate micro/nanofibrous scaffolds comprising PCL and fucoidan using an electrospinning process. We studied the electrospinability, which can vary with the weight fraction of fucoidan, and measured the mechanical and hydrophilic properties of various weight fractions (1, 2, 3, and 10 wt.%) of fucoidan. Finally, to observe the cellular behavior of the PCL/fucoidan fibrous mat as a bone tissue regeneration scaffold, total protein content, alkaline phosphatase (ALP) activity, and an alizarin red assay were determined in osteoblast-like cells (MG63).

2. Experimental procedures

2.1. Materials

PCL (M_w 80,000) was obtained from Sigma–Aldrich (St. Louis, MO, USA). Fucoidan (total polysaccharide: 62.12% and sulfate: 34.20%) was purchased from Haewon Biotech (Seoul, Korea). It was extracted from a brown seaweed *Undaria pinnatifida*. To fabricate the electrospun PCL/fucoidan biocomposite, a PCL solution was prepared by dissolving 2.4 g of PCL in 30 g of a solvent mixture of 80 wt.% methylene chloride (Junsei) and 20 wt.% dimethylformamide (Junsei). Different amounts [1 (0.33 g), 2 (0.66 g), 3 (1.0 g), and 10 (3.6 g) wt.%] of powdered fucoidan were then added; >10 wt.% fucoidan resulted in very high viscosity and inadequate electrospinning of the PCL/fucoidan solution, such that the obtained fibers exhibited string-bead shapes. Therefore, we accommodated a maximum of 10 wt.% fucoidan. Electrical conductivity of the solutions (PCL/fucoidan) was measured with a multi-parameter analyzer (C891; Consort), and surface tension was obtained using the capillary phenomenon.

2.2. Fabrication of PCL/fucoidan micro/nanofibers

A general electrospinning process was applied to generate micro/nanofibers of PCL/fucoidan. The polymer solution was placed in a 10-mL glass syringe with a 21-G needle. The feed rate of the solution (1 mL/h) was precisely controlled by a syringe pump system (KDS 230; KD Scientific). The applied electric field was 0.9–1.1 kV/cm, and a high-voltage direct current supplier (SHV300RD-50K; Convertech) was used to control the applied voltage. A constant needle-to-collector distance of 150 mm and collector rotation speed of 6.8 m/s (1300 rpm) were used. The solutions used were pure PCL, PCL with 1 wt.% fucoidan (P/F1), PCL with 2 wt.% fucoidan (P/F2), PCL with 3 wt.% fucoidan (P/F3), and PCL with 10 wt.% fucoidan (P/F10). In addition, during the electrospinning process, the temperature was set at $22 \pm 4\,^{\circ}C$ and humidity at $60 \pm 2.7\%$. A digital camera was used to measure the initial jets.

2.3. Characterization of electrospun PCL/fucoidan fiber mats

The morphology of the electrospun biocomposites was observed under an optical microscope (BX FM-32; Olympus) connected to a digital camera and under a scanning electron microscope (SEM; Sirion).

The tensile test was conducted using a universal tensile machine (Top-tech 2000; Chemilab, Seoul, Korea). The mechanical properties of the biocomposites were evaluated by measuring Young's modulus and stress at 20% of strain. The tests were performed using the biocomposites in the dry state. The specimens were cut into small strips (20 mm × 10 mm), and five samples were obtained from different sites for each electrospun mat. The stress–strain curves of the electrospun mats were recorded at a stretching speed of 1 mm/s. The thickness of the mats was measured using an optical microscope (BX41-N22, Olympus).

Fourier-transform infrared (FT-IR) spectroscopy (model 6700; Nicolet, West Point, PA, USA) was used to qualitatively measure alginate and fucoidan levels in the composites. The IR spectra represent the average of 30 scans between 500 and 4000 cm^{-1} at a resolution of 8 cm^{-1}.

To measure the water-contact angle of the biocomposites, one droplet (10 μL) of water was carefully dropped on the surface of the mats, and the contact angle was measured over time.

2.4. In vitro cell culture, ALP activity, calcium deposition, and total protein content

Electrospun mats (10 mm × 10 mm) were sterilized with 70% EtOH and UV light and placed in culture medium overnight. Osteoblast-like cells (MG63; ATCC, Manassas, VA, USA) were used to observe cellular behavior. MG63 cells were cultured in Dulbecco's modified Eagle's medium (DMEM; Hyclone, Logan, UT, USA) supplemented with 10% fetal bovine serum (Hyclone) and 1% penicillin/streptomycin (Hyclone). The cells were maintained up to passage 8 and collected by trypsin–EDTA treatment. The cells were seeded onto the mats at a density of 1×10^5 cells per sample and incubated in an atmosphere of 5% CO_2 at 37 °C. The medium was changed every other day. To assess morphology and cellular proliferation, the cells were examined by SEM after 10 days. The cells/mats were fixed in 2.5% glutaraldehyde and dehydrated through a series of graded ethanol. Dried mats were coated with gold and examined under SEM.

For MG63 cells seeded in the scaffolds for 5 and 10 days, ALP, which is a marker of osteoblast activity, was assayed by measuring the release of p-nitrophenol from p-nitrophenyl phosphate (p-NPP). The biocomposites seeded with MG63 cells were rinsed gently with phosphate-buffered saline (PBS) and incubated in Tris buffer (10 mM, pH 7.5) containing 0.1% Triton X-100 for 10 min. This was followed by adding 100 μL of the lysate to a 96-well tissue culture plate containing 100 μL of p-NPP solution, prepared using an ALP kit (procedure no. ALP-10; Sigma–Aldrich). In the presence of ALP, p-NPP is transformed to p-nitrophenol and inorganic phosphate. The ALP activity was determined by measuring the absorbance at 405 nm using a microplate reader (Spectra III; SLT-Lab Instruments, Salzburg, Austria).

Calcium mineralization was determined by alizarin red-S staining in 24-well plates. MG63 cells were cultured in DMEM containing 50 μg/mL vitamin C and 10 mM β-glycerophosphate for 10 days. The cells were then washed three times with PBS, fixed in 70% (v/v) cold ethanol (4 °C) for 1 h, and air-dried. The ethanol-fixed specimens were stained with 40 mM alizarin red-S (pH 4.2) for 1 h and washed three times with purified water. The specimens were destained with 10% cetylpyridinium chloride in 10 mM sodium phosphate buffer (pH 7.0) for 15 min. The optical density was measured at 562 nm using a Spectra III UV microplate reader.

Total protein content was measured using a bicinchoninic acid (BCA) protein assay (Pierce kit; Thermo Scientific). Cell/mat samples were assayed after culturing for 5 and 10 days. Specimens were washed with PBS and lysed with 1 mL of 0.1% Triton X-100. An aliquot of the lysate (25 μL) was added to 200 μL of BCA working reagent, and the mixture was incubated for 30 min at 37 °C. The

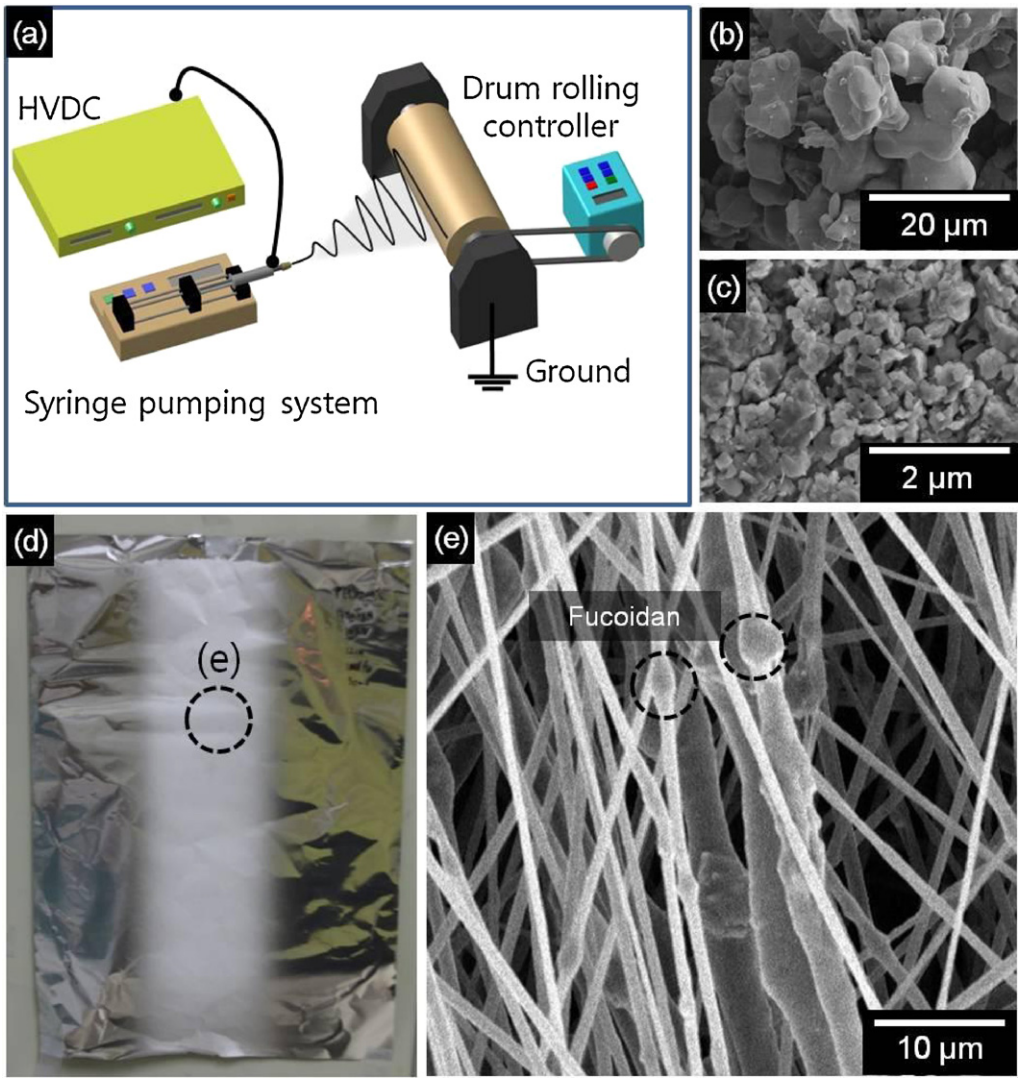

Fig. 1. (a) Schematic of an electrospinning process. (b and c) SEM images of poly(ε-caprolactone) and fucoidan powders, respectively. (d) Electrospun P/F3 on aluminum foil. (e) Magnified SEM image of (d).

absorbance at 562 nm was determined using a plate reader, and the total protein concentration was calculated using a standard curve.

2.5. Statistical analyses

All data presented are the mean ± standard deviation (SD). Statistical analyses consisted of single-factor analyses of variance (ANOVAs). The significance level was set at $P < 0.05$.

3. Results and discussion

3.1. Electrospinning process for PCL/fucoidan micro/nanofiber formation

Fig. 1(a) shows a schematic of general electrospinning. By this simple process and the mixture of PCL powder and fucoidan powder [Fig. 1(b) and (c)], we can acquire the electrospun biocomposites comprising PCL and fucoidan powders [Fig. 1(d) and (e)].

Fig. 2(a–c) shows the initial jets and stretching motion of electrospun micro/nanofibers for pure PCL and PCL/fucoidan composites (P/F2 and P/F10), respectively. As shown in the images, the length (X) of the initial jets decreased as the concentration of fucoidan in the solution increased (Table 1). This phenomenon occurred because the fucoidan increased the electrical conductivity of the P/F solution so that the highly charged fibers easily repulsed each other due to the electrostatic forces. However, the Y-length of the stretched fibers' motion in Fig. 2 can be lowered due to the high surface tension of the P/F solution.

In general, the length of the initial jets is strongly related to the final diameter of the fibers (Fridrikh, Yu, Brenner, & Rutledge, 2003). From the images in Fig. 2, we can estimate that by adding fucoidan, the diameter of the fibers can be decreased compared with pure PCL. To observe the diameter, we acquired SEM images of the electrospun fibers. Fig. 3(a–e) shows the SEM images of the final fabricated micro/nanofibers for pure PCL and P/F (1, 2, 3, and 10 wt.%), respectively. In addition, because it is well known that alignment of the fibers can affect cellular activities, such as cell alignment and proliferation, as well as mechanical properties, we measured the full width at half maximum (FWHM). As shown in Fig. 3(f), the alignment of the final fibers interfered with the injected fucoidan powders. We believe that this phenomenon occurred because injected fucoidan powders induced electrical disruption between previously deposited fibers on the electrospun mat and upcoming charged fibers. Fig. 3(g) shows the diameter of fibers for various weight fractions of fucoidan. As shown in the figure, the diameter decreased slightly as the concentration of fucoidan

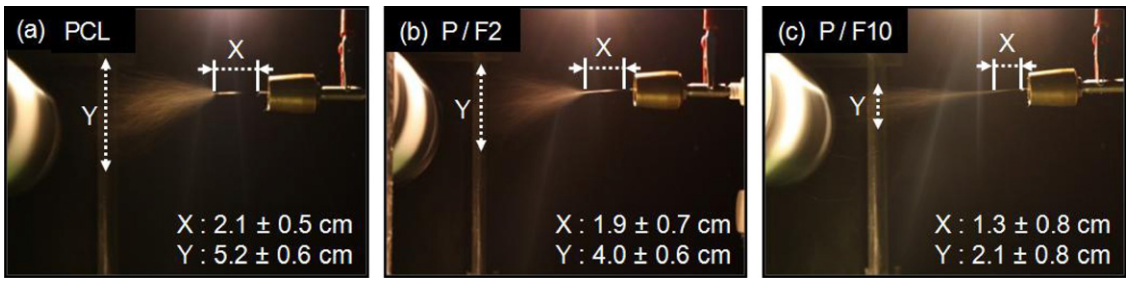

Fig. 2. Photographs of the initial jets for (a) pure PCL, (b) P/F2, and (c) P/F10. In these images, "*X*" indicates the length of an initial jet and "*Y*" indicates the dispersed length of stretched micro/nanofibers.

Table 1
Electric conductivity and surface tension of PCL/fucoidan solutions ($n = 5$).

	Pure PCL	P/F1	P/F2	P/F3	P/F10
Conductivity (ms/cm)	1.0 ± 0.2	1.1 ± 0.3	1.2 ± 0.3	1.4 ± 0.2	1.8 ± 0.1
Surface tension (kN/m)	9.1 ± 5.6	19.4 ± 2.5	23.8 ± 4.3	24.9 ± 4.6	25.2 ± 1.0

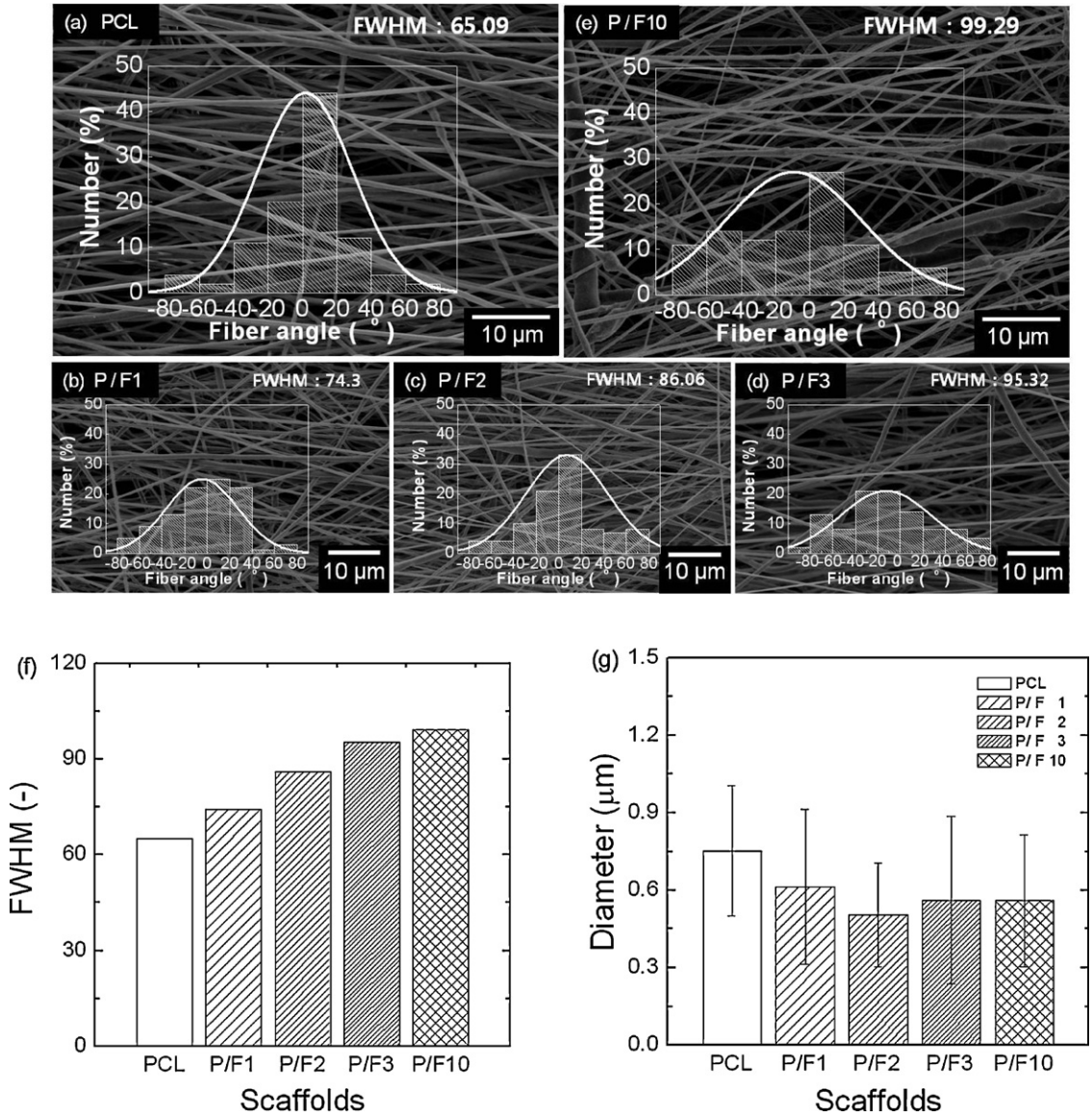

Fig. 3. (a–e) SEM images of P/F biocomposites and distribution of alignment of micro/nanofibers (FWHM: full width at half maximum). (f) Comparison of FWHM for pure PCL and each biocomposite. (g) Average diameter of the electrospun PCL/fucoidan biocomposites ($n = 100$).

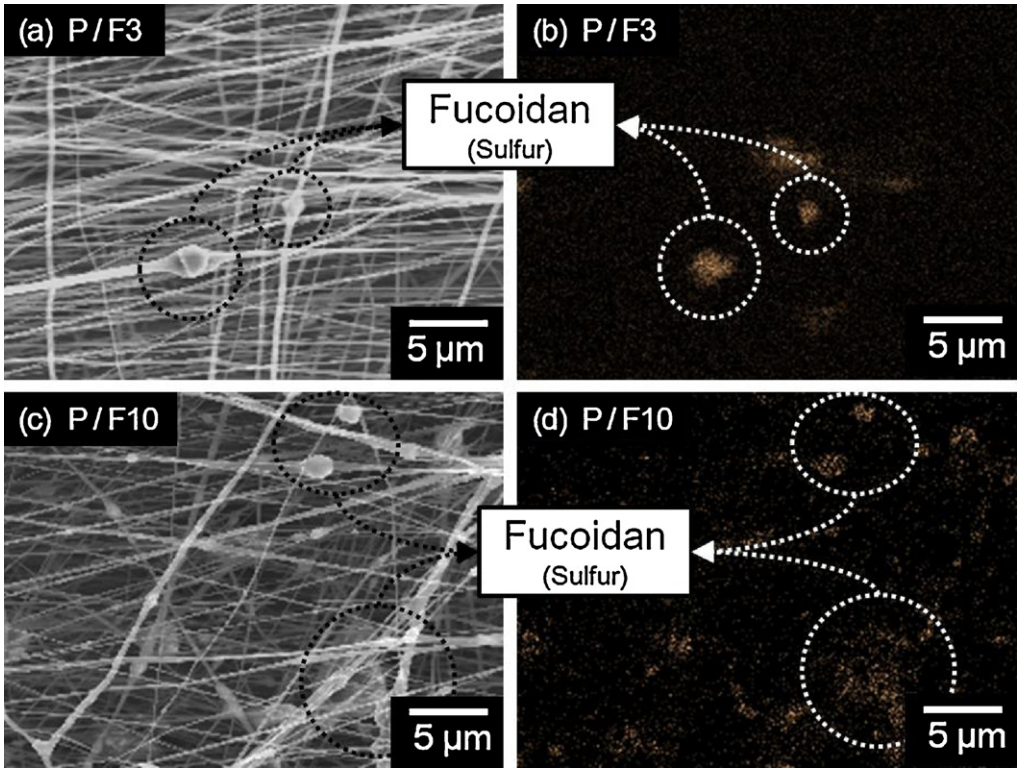

Fig. 4. SEM images of (a) P/F3 and (c) P/F10 and EDS mapping of sulfur in (b) P/F3 and (d) P/F10.

powder increased. This phenomenon occurred because of the electrical and physical changes of the P/F solutions.

3.2. Characterization of fucoidan in PCL/fucoidan fibers

Fig. 4(a–d) shows the SEM images and energy dispersive X-ray spectroscopy (EDS) mapping of sulfur, which is one of the main components of fucoidan, for two different concentrations (P/F3 wt.% and P/F10 wt.%) of fucoidan in the PCL/fucoidan fibers. EDS mapping of PCL/fucoidan micro/nanofibers shows that the fucoidan powders were well embedded, and as the concentration of fucoidan increased, the sulfur was more highly distributed in the PCL/fucoidan fibers. However, some aggregated fucoidan powders were also found at high concentrations of fucoidan. As a result of aggregation, stress concentration on the fibers under applied strain may have occurred, resulting in a decrease in mechanical properties at a high concentration of fucoidan (about 10 wt.%). More detailed mechanical analysis is presented in the next section.

3.3. Tensile test of electrospun PCL/fucoidan mats

It is well known that the mechanical properties of a scaffold are an important factor in the design of various scaffolds because neo-tissues should be sustained during the tissue regenerating process, and mechanical properties should be similar to those of the adjacent tissue in the implanted area. The stress–strain curves of the PCL/fucoidan electrospun mats were obtained using a general tensile tester at a 1-mm/s crosshead speed, and the results are presented in Fig. 5(a). Young's modulus and stress at 20% of tensile strain for the PCL/fucoidan mats are presented in Fig. 5(b). The results show that as the weight fraction of fucoidan in the PCL/fucoidan biocomposites increased, the mechanical properties (Young's modulus and stress at 20% strain) improved by as much as about 70%. However, the mechanical properties of the mat (P/F10) at 10 wt.% of fucoidan abruptly decreased. We believe that this phenomenon occurred because of the widely distributed/aggregated fucoidan powders in the mats in which applied tensile stress can be highly concentrated (Table 2).

3.4. FT-IR analysis of PCL/fucoidan mats

As shown in Fig. 6(a), to analyze the weight fraction of embedded fucoidan in the electrospun PCL/fucoidan mats, we measured the FT-IR spectra of pure PCL, pure fucoidan, and three electrospun mats (P/F1, P/F2, and P/F3). In the fucoidan spectra, the peak at 832 cm^{-1} was attributable to the bending vibration of water and the C—O—S bending vibration of the sulfate in fucoidan (Synytsya et al., 2010). Furthermore, the peak at 1220 cm^{-1} was caused by the asymmetric O=S=O stretching vibration of the sulfate esters. To measure the quantitative amount of fucoidan in the mats, we compared the two peaks (1724 cm^{-1} of PCL and 832 cm^{-1} of fucoidan) in the biocomposites. The ratio of the intensities is presented in Fig. 6(b). As shown in the figure, the intensity ratio increased linearly with the increasing weight fraction of fucoidan.

3.5. Water contact angle (WCA) of the PCL/fucoidan mats

To assess the effect of fucoidan on the hydrophilicity of the electrospun P/F fiber mats, we observed the shape of a water droplet (10 μL) of the biocomposites with various weight fractions of fucoidan during 30 min [Fig. 7(a)]. The contact angle of the droplet for various P/F mats was measured and compared with that of the mat spun from pure PCL (initial angle, 122°; after 30 min, 117°). At the initial time point, the WCA values of the biocomposites were similar to that of the pure PCL mat. However, over time, the WCAs of the biocomposites decreased, indicating that the hydrophilicity of the P/F improved with the addition of fucoidan. In particular, the improvement was dramatic when the addition of

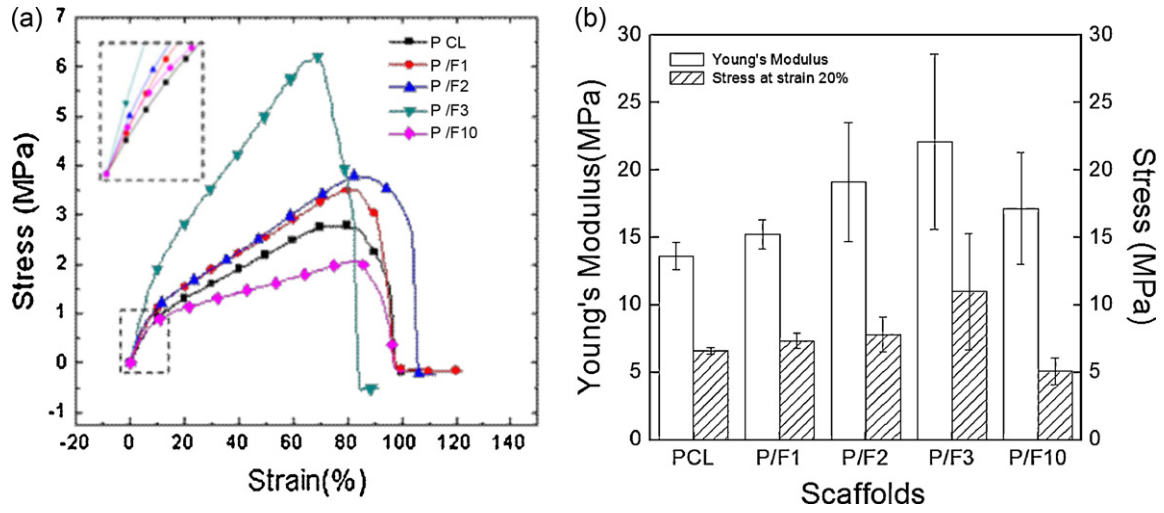

Fig. 5. Young's modulus and stress at 20% strain for various biocomposites; (a) stress–strain curves and (b) measured Young's modulus and stress at 20% strain ($n = 5$).

Table 2
Young's modulus and stress at 20% strain of PCL/fucoidan micro/nanofibrous mats ($n = 5$).

	Pure PCL	P/F1	P/F2	P/F3	P/F10
Young's modulus (MPa)	13.6 ± 1.0	15.2 ± 1.1	19.1 ± 4.4	22.1 ± 6.5	17.2 ± 4.2
Stress (MPa)	6.3 ± 0.8	7.3 ± 1.5	8.2 ± 2.7	11.6 ± 4.2	5.1 ± 2.1

fucoidan was greater than 3 wt.% in the PCL/fucoidan. The change in the WCA for various time periods is shown in Fig. 7(b). The WCA of the PCL/fucoidan was time-dependent, and although the initial contact angle of the biocomposites was similar to that of the pure PCL mat, the WCA gradually decreased as the weight fraction of fucoidan increased.

3.6. In vitro cell culture, ALP activity, and calcium deposition

To assess the effects of fucoidan on cellular responses, SEM images of pure PCL and biocomposites (P/F2 and P/F10) cultured with MG63 cells were taken at 10 days [Fig. 8(a–f)]. Cell morphology and proliferation could be observed in the SEM images. The images indicated that the proliferated osteoblast-like cells (MG63) well covered the surface of the electrospun pure PCL and biocomposites. However, in the fucoidan-embedded electrospun mats, the cells were more agglomerated, and this phenomenon was accelerated with higher concentrations of fucoidan. As shown in Fig. 8(g), the relative ALP activity was measured after culturing for 5 and 10 days. The data were normalized to the relative total protein content, which was obtained by dividing the total protein content of the PCL/fucoidan biocomposites by that of pure PCL (Table 3). To compare the biocomposites with the pure PCL, the data were divided by the pure PCL result so that the ALP activity of the biocomposites was displayed relative to the pure PCL. At days 5 and 10, the cells on the biocomposites with fucoidan exhibited considerably higher ALP levels compared with those of the pure PCL. In addition, alizarin red-S (ARS) has been used to determine the levels of calcium minerals. The optical density value of the biocomposites was normalized to the relative total protein content, like the previous ALP activity results [Fig. 8(h)]. For all biocomposites, the relative ARS intensities of the biocomposites with fucoidan were higher than that of the pure PCL mat. We think that the increase of ALP level and ARS intensities could be because of the

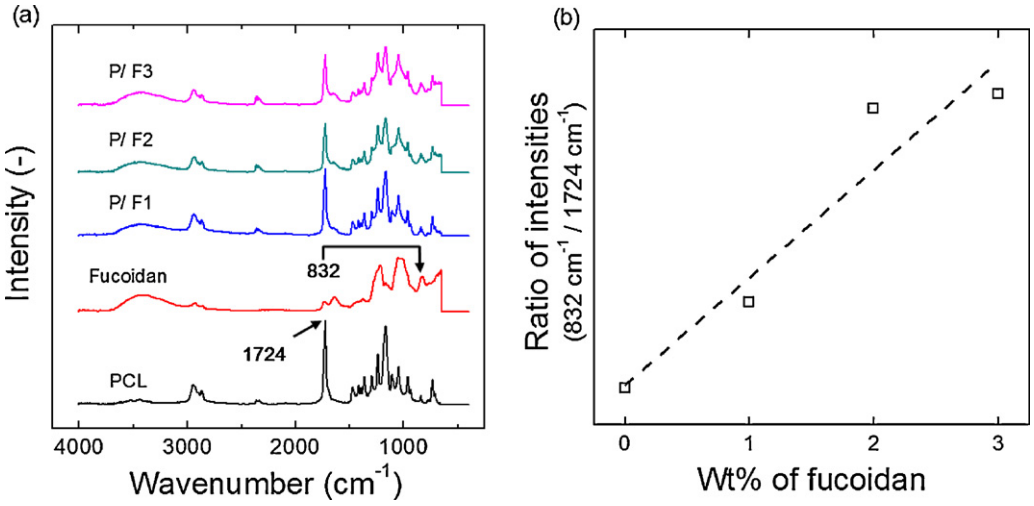

Fig. 6. (a) FT-IR spectra of pure PCL and P/F biocomposites for various weight fractions of fucoidan (1, 2, and 3 wt.%). (b) Ratio of 832–1724 cm^{-1} for various weight fractions of fucoidan.

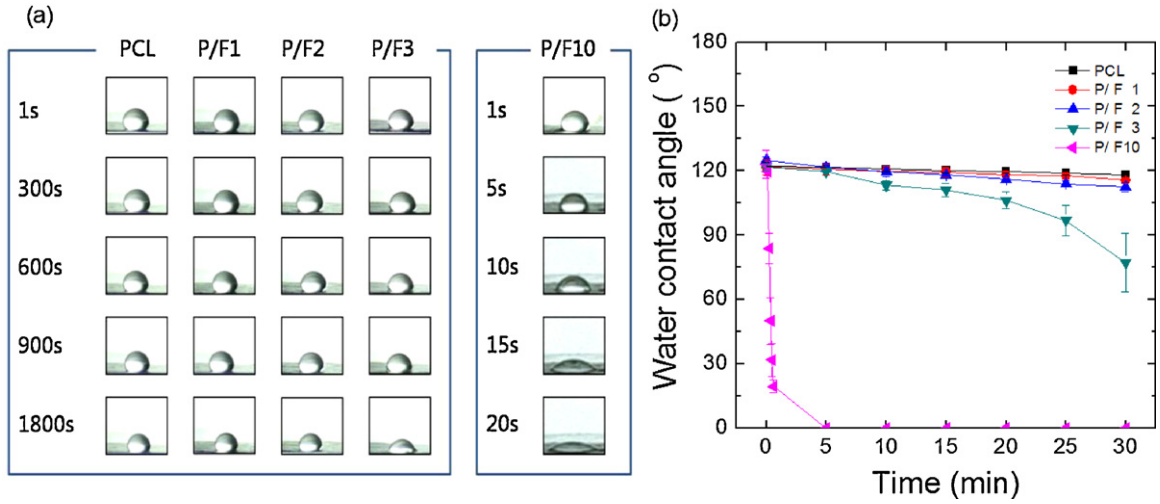

Fig. 7. (a) Transient change in a water droplet (10 μL) on the various biocomposites and (b) measured water contact angle of each biocomposite ($n = 5$).

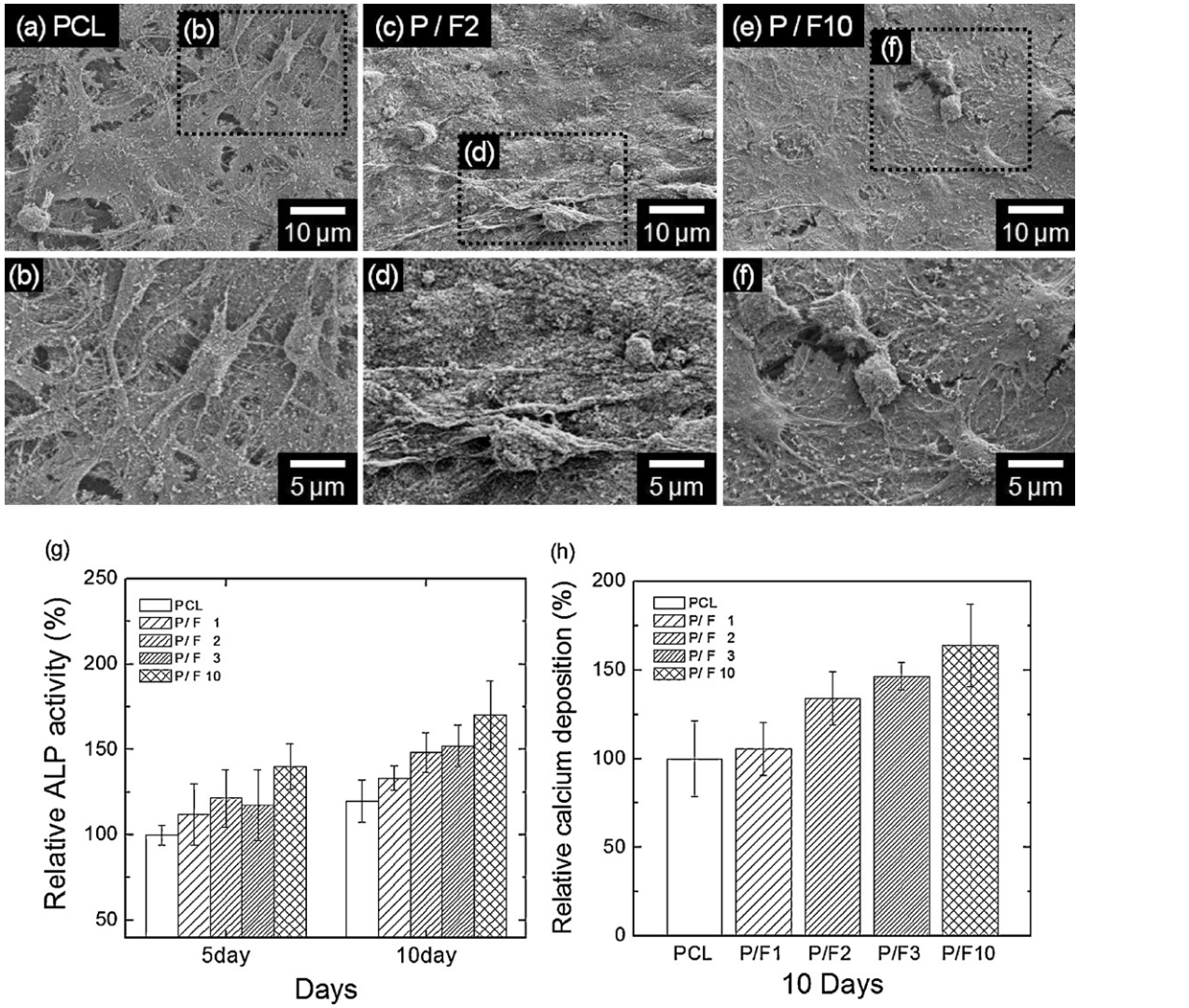

Fig. 8. SEM micrographs of MG63 cells cultured on mats composed of (a and b) pure PCL, (c and d) P/F2, and (e and f) P/F10 for 10 days. (f) Relative alkaline phosphatase (ALP) activity of MG63 cells cultured on mats composed of pure PCL and biocomposites for 5 and 10 days, and (g) relative calcium deposition for pure PCL and biocomposites for 10 days ($n = 5$).

Table 3
Relative total protein content after cell culture for 5 days and 10 days ($n = 5$).

	PCL	P/F1	P/F2	P/F3	P/F10
5 days (%)	100 ± 14	107 ± 13	115 ± 17	136 ± 13	135 ± 10
10 days (%)	100 ± 10	100 ± 14	101 ± 8	110 ± 8	119 ± 8

fucoidan release from the biocomposites. In previous our work, we fabricated solid freefrom fabricated PCL/fucoidan scaffolds (Jin & Kim, 2011). In the results, the calcium deposition was proportionally increased with the fucoidan release from the scaffolds. In this study, although we did not measure the fucoidan release from the electrospun biocomposites, we can estimate that the fucoidan can be released from the biocomposites. Also, according to several researchers, the fucoidan has been known that it can significantly enhance the expression of osteogenesis-specific marker genes (ALP, osteopontin, type I collagen, Runt-related transcription factor 2, and osteocalcin) (Changotade et al., 2008; Park, Lee, Lim, & Lee, 2011). From these several works, we can estimate that the released fucoidan may improve the ALP activity and induce calcium deposition. Based on these results, we can suggest that electrospun PCL/fucoidan mats may be a potential biomaterial for bone tissue regeneration.

4. Conclusion

Using a general electrospinning process, we obtained PCL/fucoidan micro/nanofibrous mats (diameter range, $0.5 \pm 0.4\,\mu m$) with various fucoidan contents (1, 2, 3, and 10 wt.%). The fibrous biocomposites exhibited marked hydrophilicity when the weight fraction of fucoidan was >3 wt.% and had a higher Young's modulus than the pure PCL mat. However, at a high weight fraction (about 10 wt.%) of fucoidan in the PCL/fucoidan mats, the agglomerated fucoidan induced stress concentration in the tensile mode so that a low Young's modulus and stress at 20% strain were acquired. With regard to biological activities, the addition of fucoidan in the biocomposites stimulated cellular activities, including ALP activity and calcium mineralization. However, although the bioactivities were improved by increasing the fucoidan fraction, low electrospinability and low mechanical properties resulted. These results show that the weight fraction of fucoidan in the electrospun biocomposites should be optimized with consideration of biological activities and mechanical properties. Finally, if we can address the aforementioned problems, electrospun PCL/fucoidan fibrous mats may be a potential biomaterial for bone tissue regeneration.

Acknowledgements

This research was financially supported by the Ministry of Education, Science, and Technology (MEST) and the National Research Foundation of Korea (NRF) through the Human Resource Training Project for Regional Innovation, and was supported by the Basic Science Research Program through the National Research Foundation of Korea (NRF) funded by the Ministry of Education, Science, and Technology (grant no. 2011-0004097).

References

Changotade, S. I., Korb, G., Bassil, J., Barroukh, B., Willig, C., Colliec-Jouault, S., et al. (2008). Potential effects of a low-molecular-weight fucoidan extracted from brown algae on bone biomaterial osteoconductive properties. *Journal of Biomedical Materials Research A*, *87*, 666–675.

Chen, G., Ushida, T., & Tateishi, T. (2002). Scaffold design for tissue engineering. *Macromolecular Bioscience*, *2*, 67–77.

Fridrikh, V., Yu, J. H., Brenner, M. P., & Rutledge, G. C. (2003). Controlling the fiber diameter during electrospinning. *Physical Review Letters*, *90*, 144502.

Glowacki, J., & Mizuno, S. (2008). Collagen scaffolds for tissue engineering. *Biopolymers*, *89*, 338–344.

Hirose, Y., Amiya, T., Hirokawa, Y., & Tanaka, Y. (1987). Phase transition of submicron gel beads. *Macromolecules*, *20*, 1342–1344.

Hollister, S. J. (2005). Porous scaffold design for tissue engineering. *Nature Materials*, *4*, 518–524.

Hubbell, J. A., & Langer, R. (1995). Tissue engineering. *Chemical & Engineering News*, *73*, 42–54.

Hutmacher, D. W. (2001). Scaffold design and fabrication technologies for engineering tissues – State of the art and future perspectives. *Journal of Biomaterials Science Polymer Edition*, *12*, 107–124.

Jin, G., & Kim, G. H. (2011). Rapid-prototyped PCL/fucoidan composite scaffolds for bone tissue regeneration: Design, fabrication and physical/biological properties. *Journal of Materials Chemistry*, *21*, 17710–17718.

Kretlow, J. D., & Mikos, A. G. (2008). From material to tissue: Biomaterial development, scaffold fabrication and tissue engineering. *AIChE Journal*, *54*, 3048–3067.

Langer, R., & Vacanti, J. P. (1993). Tissue engineering. *Science*, *260*, 920–926.

Langer, R., & Vacanti, J. P. (1995). Artificial organ. *Scientific America*, *273*, 130.

Li, B., Lu, F., Wei, X., & Zhao, R. (2008). Fucoidan: Structure and bioactivity. *Molecules*, *13*, 1671–1695.

Li, W. J., Laurencin, C. T., Caterson, E. J., Tuan, R. S., & Ko, F. K. (2002). Electrospun nanofibrous structure: A novel scaffold for tissue engineering. *Journal of Biomedical Materials Research*, *60*, 613–621.

Luyt, C., Meddahi-Pelle, E., Ho-Tin-Noe, A., Colliec-Jouault, B., Guezennec, S., Louedec, J., et al. (2003). Low-molecular-weight fucoidan promotes therapeutic revascularization in a rat model of critical hindlimb ischemia. *The Journal of Pharmacology and Experimental Therapeutics*, *305*, 24–30.

Ma, Z., He, W., Yong, T., & Ramakrishna, S. (2005). Grafting of gelatin on electrospun poly(caprolactone) nanofibers to improve endothelial cell spreading and proliferation and to control cell orientation. *Tissue Engineering*, *11*, 1149–1158.

Ma, Z. W., Kotaki, M., Inai, R., & Ramakrishna, S. (2005). Potential of nanofiber matrix as tissue-engineering scaffolds. *Tissue Engineering*, *11*, 101–109.

Nakamura, S., Nambu, M., Ishizuka, T., Hattori, H., Kanatani, Y., Takase, B., et al. (2008). Effect of controlled release of fibroblast growth factor-2 from chitosan/fucoidan micro complex-hydrogel on in vitro and in vivo vascularization. *Journal of Biomedical Materials Research Part A*, *85*, 619–627.

Nerem, R. M., & Sambanis, A. (1995). Tissue engineering: From biology to biological substitutes. *Tissue Engineering*, *1*, 3–13.

Park, S.-J., Lee, K. W., Lim, D.-S., & Lee, S. (2011). The sulfated polysaccharide fucoidan stimulates osteogenic differentiation of human adipose-derived stem cells. *Stem Cells & Development*, http://dx.doi.org/10.1089/scd.2011.0521

Ratner, B. D., Hoffman, A. S., Schoen, F. J., & Lemons, J. E. (1996). *Biomaterials science: An introduction to materials in medicine*. Academic Press.

Sachlos, E., & Czernuszka, J. T. (2003). Making tissue engineering scaffolds work. Review on the application of solid freeform fabrication technology to the production of tissue engineering scaffolds. *European Cells and Materials*, *5*, 29–40.

Senni, K., Pellat, B., Gogly, B., Blondin, C., Jozefonvicz, J., Letourneur, D., Colliec-Jouault, S., Durand, P., & Sinquin, C. (2003). US Patent 6,559,131.

Shin, M., Yoshimoto, H., & Vacanti, J. P. (2004). *In vivo* bone tissue engineering using mesenchymal stem cells on a novel electrospun nanofibrous scaffold. *Tissue Engineering*, *10*, 33–41.

Synytsya, A., Kim, W. J., Kim, S. M., Pohl, R., Synytsya, A., Kvasnicka, F., et al. (2010). Structure and antitumour activity of fucoidan isolated from sporophyll of Korean brown seaweed *Undaria pinnatifida*. *Carbohydrate Polymers*, *81*, 41–48.

Teo, W. E., & Ramakrishna, S. (2006). A review on electrospinning design and nanofibre assemblies. *Nanotechnology*, *17*, R89–R106.

Yang, S., Leong, K. F., Du, Z., & Chua, C. K. (2001). The design of scaffolds for use in tissue engineering. Part I. Traditional factors. *Tissue Engineering*, *7*, 679–689.

Yoo, J. J., & Lee, I. W. (1998). *Tissue Engineering: Concepts and Application*. Seoul: Korea Medical Publications.

Yoshimoto, H., Shin, Y. M., Terai, H., & Vacanti, J. P. (2003). A biodegradable nanofiber scaffold by electrospinning and its potential for bone tissue engineering. *Biomaterials*, *24*, 2077–2082.

Zeltinger, J., Sherwood, J. K., Graham, D. A., Mueller, R., & Griffith, L. G. (2001). Effect of pore size and void fraction on cellular adhesion, proliferation and matrix deposition. *Tissue Engineering*, *7*, 557–572.